HHS Public Access

Author manuscript

Cell Rep. Author manuscript; available in PMC 2018 August 10.

Published in final edited form as:

Cell Rep. 2018 July 10; 24(2): 312–319. doi:10.1016/j.celrep.2018.06.039.

A Hepatocyte FOXN3-α Cell Glucagon Axis Regulates Fasting Glucose

Santhosh Karanth[1,2], **J.D. Adams**[3], **Maria de los Angeles Serrano**[1,4], **Ezekiel B. Quittner-Strom**[1,5], **Judith Simcox**[6], **Claudio J. Villanueva**[6], **Lale Ozcan**[7], **William L. Holland**[1,5,6], **H. Joseph Yost**[1,4,8], **Adrian Vella**[3], and **Amnon Schlegel**[1,2,5,6,9,*]

[1]University of Utah Molecular Medicine Program, University of Utah School of Medicine, Salt Lake City, UT, USA

[2]Department of Internal Medicine, Division of Endocrinology, Metabolism and Diabetes, University of Utah School of Medicine, Salt Lake City, UT, USA

[3]Department of Internal Medicine, Division of Endocrinology, Diabetes, Metabolism, and Nutrition, Mayo Clinic College of Medicine, Rochester, MN, USA

[4]Department of Neurobiology and Anatomy, University of Utah School of Medicine, Salt Lake City, UT, USA

[5]Department of Nutrition and Integrative Physiology, University of Utah College of Health, Salt Lake City, UT, USA

[6]Department of Biochemistry, University of Utah School of Medicine, Salt Lake City, UT, USA

[7]Department of Medicine, Division of Molecular Medicine, Columbia University Medical Center, New York, NY, USA

[8]Department of Pediatrics, University of Utah School of Medicine, Salt Lake City, UT, USA

[9]Lead Contact

Abstract

SUMMARY—The common genetic variation at rs8004664 in the *FOXN3* gene is independently and significantly associated with fasting blood glucose, but not insulin, in non-diabetic humans. Recently, we reported that primary hepatocytes from rs8004664 hyperglycemia risk allele carriers

*Correspondence: amnons@u2m2.utah.edu.

AUTHOR CONTRIBUTIONS

Conceptualization, S.K., L.O., W.L.H., A.V., and A.S.; Methodology, S.K., M.d.l.A.S., and A.S.; Software, S.K., J.D.A., and M.d.l.A.S.; Validation, S.K., J.D.A., M.d.l.A.S., J.S., and A.S.; Formal Analysis, S.K., J.D.A., M.d.l.A.S., and J.S.; Investigation, S.K., J.D.A., M.d.l.A.S., E.B.Q.-S., and J.S.; Resources, C.J.V., L.O., H.J.Y., A.V., and A.S.; Data Curation, S.K., J.D.A., M.d.l.A.S., A.V., and A.S.; Writing – Original Draft, S.K. and A.S.; Writing – Re-view & Editing, S.K., J.D.A., M.d.l.A.S., J.S., L.O., A.V., and A.S.; Visualization, S.K., J.D.A., M.d.l.A.S., A.V., and A.S.; Supervision, C.J.V., L.O., W.L.H., H.J.Y., A.V., and A.S.; Project Administration, A.S.; Funding Acquisition, C.J.V., L.O., W.L.H., H.J.Y., A.V., and A.S.

DECLARATION OF INTERESTS

The authors declare no competing interests.

SUPPLEMENTAL INFORMATION

Supplemental Information includes Supplemental Experimental Procedures, two figures, and three tables and can be found with this article online at https://doi.org/10.1016/j.celrep.2018.06.039.

have increased FOXN3 transcript and protein levels and liver-limited overexpression of human FOXN3, a transcriptional repressor that had not been implicated in metabolic regulation previously, increases fasting blood glucose in zebrafish. Here, we find that injection of glucagon into mice and adult zebrafish decreases liver Foxn3 protein and transcript levels. Zebrafish *foxn3* loss-of-function mutants have decreased fasting blood glucose, blood glucagon, liver gluconeogenic gene expression, and α cell mass. Conversely, liver-limited overexpression of *foxn3* increases α cell mass. Supporting these genetic findings in model organisms, non-diabetic rs8004664 risk allele carriers have decreased suppression of glucagon during oral glucose tolerance testing. By reciprocally regulating each other, liver FOXN3 and glucagon control fasting glucose.

In Brief—Karanth et al. find that glucagon lowers liver expression of Foxn3. Deletion of the Foxn3 gene decreases fasting blood glucose and the number of glucagon-producing α cells in the primary islet of zebrafish. Human carriers of the hyperglycemia risk allele of FOXN3 gene fail to suppress glucagon during oral glucose challenge.

Graphical Abstract

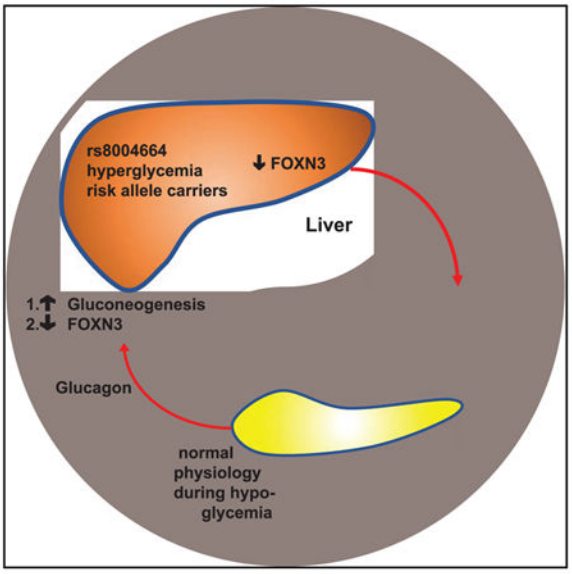

INTRODUCTION

Type 2 diabetes mellitus (DM2) has reached pandemic proportions (Danaei et al., 2011). The last decade has witnessed a wealth of human genomics findings that can shed diagnostic, prognostic, and therapeutic light on this disease. Most of the approximately 100 loci identified in population-based studies as being associated with DM2 appear to act primarily, albeit not exclusively, in the development, survival, and function of the insulin-producing β cell of the endocrine pancreas (Fuchs-berger et al., 2016). Additionally, defects in insulin action in multiple tissues also have complex physiological effects and contribute to frank hyperglycemia (Lotta et al., 2017). Beyond several loci that disrupt β cells, an understanding of the contributions of individual population-genetics-identified DM2 loci is lacking for the vast majority of polymorphisms (Bonnefond and Froguel, 2015; Sanghera and Blackett,

2012). This void affords an opportunity to elucidate fundamental mechanisms of immediate clinical relevance for diagnosis and therapy through human physiological investigations and animal model studies.

The *FOXN3* locus merits attention because of the statistically significant and independent association of the SNP rs8004664, which occurs in the first intron of human *FOXN3*, with fasting blood glucose, but not with fasting insulin, in non-diabetic subjects (Manning et al., 2012). Recently, we found that carriers of the rs8004664 hyperglycemia risk allele show greater expression of the transcriptional repressor FOXN3 in hepatocytes (Karanth et al., 2016). Forced overexpression of both human *FOXN3* and zebrafish *foxn3* cDNAs in zebrafish livers is sufficient to increase fasting glucose, in part, by suppressing expression of the master transcriptional regulator of glucose utilization, *Myc*, and by driving gluconeogenesis (Karanth et al., 2016). Because both the transcripts and proteins encoded by FOXN3 orthologs in zebrafish and rat livers are downregulated during fasting (Karanth et al., 2016), our results suggest the hypothesis that the rs8004664 risk allele drives sustained expression of FOXN3 during fasting, and this pathological increase in FOXN3 contributes to increased fasting blood glucose.

Here, we performed glucagon challenge in mice and zebrafish and found Foxn3 protein and transcript were decreased. These findings and previous reports that *Xenopus* embryos injected with anti-*foxn3* morpholino oligonucleotides and *Foxn3*$^{-/-}$ mice die at early stages from craniofacial defects (Samaan et al., 2010; Schuff et al., 2007) prompted us to prepare a viable *foxn3* loss-of-function zebrafish mutant allele to test the hypothesis that Foxn3 is a critical factor participating in fasting liver metabolism. The *foxn3* loss-of-function zebrafish mutants show decreased fasting blood glucose and glucagon on a normal diet and have fewer α cells in the principal islet. Conversely, animals overexpressing *foxn3* in the liver show increased numbers of α cells in the principal islet and higher blood glucagon. Finally, we performed oral glucose tolerance tests in non-diabetic adult humans genotyped for the rs8004664 variant and found that the homozygous risk allele carriers have nominally higher fasting blood glucose and show significantly blunted suppression of glucagon during an oral glucose tolerance test. These results indicate that hepatic Foxn3 is regulated by glucagon and, in turn, regulates fasting blood by modulating glucagon.

RESULTS

Glucagon Signaling Regulates Liver Foxn3 Expression in Mice and Zebrafish

Previously, we found that, in fasted zebrafish and rats (Karanth et al., 2016), Foxn3 protein and transcripts decrease. These findings raised the hypothesis that glucagon signaling in liver regulates Foxn3 expression. To test this possibility, we performed Glucagon challenge in mice (Figure 1A; Table S1) and measured Foxn3 protein at the conclusion of the study. Glucagon injection caused a 30% decrease in mouse Foxn3 protein after 20 min (Figure 1B). The *Foxn3* mRNA did not decrease during this period (not shown). We then treated primary mouse hepatocytes with glucagon. Recapitulating our whole-animal results, glucagon treatment decreased hepatocyte Foxn3 levels (Figure 1C).

To test whether glucagon might regulate *foxn3* transcript abundance hours after administration, we returned to the zebrafish model. We injected adult zebrafish with human glucagon and observed a rise in blood glucose in both sexes after two hours (Figure 1D). Livers were harvested from animals after blood collection, and *phos-phoenolpyruvate carboxykinase 1* (*pck1*), which is induced in other organisms by glucagon, and *foxn3* transcripts were measured (Table S2). The *pck1* transcript was induced by glucagon administration, and *foxn3* transcript was decreased in both sexes (Figure 1E). Finally, we measured *foxn3* transcripts in zebrafish injected with vehicle or streptozotocin (STZ) to gauge the rapidity of *foxn3* downregulation in response to unopposed endogenous glucagon action. Twenty-four hours following a single STZ treatment, blood glucose levels were significantly increased from 67 ± 6 mg/dL to 270 ± 34 mg/dL ($p < 0.01$; Safavi-Hemami et al., 2015); liver *foxn3* transcript abundance in these animals was decreased by STZ treatment (Figure 1F).

Deletion of Foxn3 Decreases Fasting Blood Glucose and Glucagon and Lowers Liver Gluconeogenic Gene Expression in Zebrafish

We prepared a *foxn3* in-frame deletion mutant (strain *z111*) using CRISPR/Cas9 to assess the impact on glucose metabolism (Figure 2A). Homozygous *foxn3*$^{z111/z111}$ mutants were never recovered from in-crosses of heterozygous carriers: *foxn3*$^{z111/z111}$ mutants died before the mid-blastula transition (not shown). This death is consistent with the perinatal lethality seen in homozygous *Foxn3* mutant mice and *Xenopus* embryos injected with anti-Foxn3 morpholinos (Samaan et al., 2010; Schuff et al., 2007). Surviving progeny of a heterozygous *foxn3*$^{z111/+}$ mutant in-cross were indistinguishable in terms of developmental staging and were identified in the expected ratio. Heterozygous *foxn3*$^{z111/+}$ mutant adults were morphologically normal (Table S3) and fertile. They also showed strong downregulation of *foxn3* transcript abundance in liver, where expression is normally high (Figure 2B; Table S2). A reciprocal increase in *mycb* expression was noted in this organ, confirming de-repression of this direct Foxn3 target (Karanth et al., 2016). These results suggested that we prepared a null *foxn3* allele, and heterozygous carriers had strong downregulation of *foxn3* expression and function.

When maintained on a standard diet, both female and male *fox3*$^{z111/+}$ mutant adults had significantly decreased fasting blood glucose compared to wild-type (WT) siblings (Figure 2C). These results confirm the increased fasting blood glucose we observed in adult animals overexpressing zebrafish *foxn3* or human *FOXN3* in the liver (*Tg(fabp10a:foxn3,EGFP)*^{z106} and *Tg*(*fabp10a:FOXN3,EGFP*)^{z107}, respectively; Karanth et al., 2016). To test whether the decrease in fasting blood glucose seen in *foxn3*$^{z111/+}$ mutants might reflect altered gluconeogen-esis, we crossed *foxn3*$^{z111/+}$ mutants to the *Tg*(*pck1:Luc2; cryaa:mCherry*)^{s952} transgenic reporter line, which carries a cDNA encoding Luciferase 2 under the control of zebrafish *pck1* promoter sequences (Gut et al., 2013), and compared the reporter activity in WT and *foxn3*$^{z111/+}$ mutants. The reporter activity in *foxn3*$^{z111/+}$; *Tg*(*pck1:Luc2;cryaa:mCherry*)^{s952} larvae was lower than WT (i.e., *foxn3*$^{+/+}$; *Tg*(*pck1:Luc2;cryaa:mCherry*)^{s952}) larvae (Figure 2D). This decrease in reporter activity was reversed when liver *foxn3* expression was restored in *foxn3*$^{z111/+}$ mutants: *foxn3*$^{z111/+}$; *Tg*(*fabp10a:foxn3,EGFP*)^{z106}; *Tg*(*pck1:Luc2;cryaa:mCherry*)^{s952} larvae had higher reporter

activity. Next, to assess the cell-autonomous role of *foxn3* in regulating blood glucose, we measured blood glucose in *foxn3*$^{+/z111}$ and *foxn3*$^{+/z111}$; *Tg*(*fabp10a:fox3,EGFP*)^{z106} adults (Figure 2E). Introduction of a liver-limited *foxn3* transgene increased fasting blood glucose in *foxn3*$^{+/z111}$ mutants. These results raised the possibility that liver Foxn3 regulates blood glucagon concentrations. Thus, we measured blood glucagon in fasting WT and *foxn3*$^{+/z111}$ adults. Figure 2F shows that *foxn3*$^{+/z111}$ animals have lower blood glucagon than WT animals.

Liver FOXN3 Regulates α Cell Mass in Zebrafish

Next, we assessed α cell mass with imaging of the principal islets in larvae to test the possibility that liver *foxn3* expression reciprocally modulates the abundance of glucagon-producing cells. To this end, we crossed *foxn3*$^{z111/+}$ mutants to the *Tg*(*gcga:GFP*)^{ia1} line, a fluorescent reporter of *glucagon-a*-expressing cells in the principal islet (Zecchin et al., 2007). We found that, compared to WT larvae, *foxn3*$^{z111/+}$ mutants had fewer GFP-expressing cells (Figures 3A, 3B, and S1), but not fewer GFP-ex-pressing cells in the islets that were proliferating, as assessed by histone H3(Ser10) phosphorylation (Figures 3B and S1). When we compared *Tg*(*gcga:GFP*) ^{ia1} larvae to *Tg*(*gcga:GFP*)^{ia1}; *Tg*(*fabp10a:FOXN3,EGFP*)^{z107} larvae, we found that forced overexpression of FOXN3 in the liver was sufficient to increase the number of *glucagon-a*-expressing cellsand the number of proliferating cells in the principal islet (Figures 3C, 3D, and S1).

The rs8004664 Risk Allele Is Associated with Decreased Suppression of Glucagon in an Oral Glucose Tolerance Test

Finally, we took a human physiological approach to understanding the effect of the rs8004664 risk allele (A) on glucose metabolism. A cohort of 402 non-diabetic adults (males = 165) underwent a 2-hr, 7-sample oral glucose tolerance test with measurement of glucose, insulin, C-peptide, and glucagon (Table 1). The rs8004664 risk allele was nominally associated with fasting blood glucose (Table 2). Insulin, C-peptide, other glucose parameters, and indices of insulin secretion and action derived from these measurements were not associated with the rs8004664 risk allele. Although fasting and nadir glucagon and the glucagon area under the curve were not associated with the rs8004664 risk allele, suppression of glucagon (quanti-fled as area below baseline) was impaired in subjects with 2 copies of the risk allele at rs800664 after adjustment for age, sex, and weight (Table 2; Figure S2). Taken with our animal physiology results, these human observations suggest that Foxn3 regulates fasting blood glucose by responding to and feeding back on glucagon signaling (Figure 3E).

DISCUSSION

We previously demonstrated that FOXN3 represses hepatic glucose utilization and promotes gluconeogenesis. Here, we showed that liver FOXN3 is regulated by and regulates glucagon. Taken with our previous work in a gain-of-function model (and additional gain-of-function experiments presented here), we posit that FOXN3 coordinates glucose utilization and production through cell-autonomous and non-autonomous routes. The mechanism through which liver FOXN3 directs α cell mass expansion and glucagon secretion will be important

to establish, because it may reveal aspects of DM2 pathogenesis of diagnostic and therapeutic relevance. Namely, liver FOXN3 may influence one or more of the many intrinsic, paracrine, endocrine, and neuronal inputs that control glucagon secretion (Campbell and Drucker, 2015; Gromada et al., 2007).

Because the rs8004664 risk allele is associated with increased fasting blood glucose in non-diabetic subjects, but not with hy-perinsulinemia, FOXN3 overexpression might contribute to the early steps of DM2 pathogenesis that center on prolonged glucagon action. Indeed, in a large cohort of subjects that includes persons with normal glucose tolerance, hyperinsulinemic pre-diabetics, and hyperinsulinemic frank diabetics, failure to suppress glucagon during an oral glucose tolerance test is observed in the latter two groups but is more severe in frank diabetics (Fæch et al., 2016). This observation is consistent with our findings in non-diabetic subjects carrying two risk alleles at the rs8004664 locus, where there is blunted suppression of glucagon following oral glucose challenge. Examining glucagon suppression during oral glucose tolerance testing in additional non-diabetic, insulin-resistant, or frankly diabetic subjects will help to fully assess the role of the rs8004664 risk allele in disease progression. We hypothesize that rs8004664 risk allele carriers will have progressively higher basal glucagon across these three categories (i.e., highest in frankly diabetic subjects) and that oral glucose challenge will be progressively less effective in suppressing glucagon. Assuming similar variation in fasting and nadir glucagon concentrations as those observed in the current cohort, 800 subjects with the G|G genotype at rs8004664 and 800 subjects with the A|A genotype at rs8004664 would provide 80% power to detect an ~10% difference in fasting and nadir glucagon concentrations. 1,600 subjects in each group would provide similar power to detect an ~6% difference. Similarly, we predict that modulating liver Foxn3 gene dose in mice will also allow us to correlate the suppression of glucagon by glucose to α cell mass.

The role of liver FOXN3 in regulating α cell mass and proliferation will require further attention as well. When *Gcgr* is deleted in mouse (Conarello et al., 2007; Gelling et al., 2003; Longuet et al., 2013; Parker et al., 2002; Sørensen et al., 2006) or when *gcgra* and *gcgrb* are simultaneously deleted in zebrafish (Li et al., 2015), hyperglucagonemia and α cell proliferation occur. In both animal models of absolute glucagon resistance, α cell mass is expanded to compensate for the lack of glucagon signaling, which is marked by improved glucose tolerance. Somewhat surprisingly, a single homozygous human carrier of a loss-of-function *GCGR* mutation developed massive α cell hyperplasia and hyperglucagonemia, but he did not have decreased fasting blood glucose or show improved glucose tolerance (Larger et al., 2016). Characterization of additional human carriers of *GCGR* mutations will give us a more complete understanding of the life-long role of this signaling pathway in regulating glucose and nitrogen metabolism (Holst et al., 2017).

The observation that WT pancreatic islets undergo α cell hyperplasia when transplanted into liver-limited *Gcgr*-deficient mice prompted a search for a factor that regulates α cell mass (Longuet et al., 2013). The circulating factors released by the liver to promote mTor-directed α cell proliferation when Gcgr is deleted or pharmacologically antagonized in mouse liver are amino acids that were not used for gluconeogenesis (Bozadjieva et al., 2017; Dean et al., 2017; Galsgaard et al., 2018; Kim et al., 2017; Solloway et al., 2015). It is possible that

Foxn3 modulates amino acid metabolism in the liver, alters production of other α cell trophic factors, or both.

Another possibility is that liver Foxn3 promotes β cell dedifferentiation and subsequent α cell differentiation (Cinti et al., 2016; Talchai et al., 2012). We hope to test specifically whether liver Foxn3 promotes conversion of β cells to α cells by driving paracrine glucagon signaling (Ye et al., 2015). Also, we will test whether liver Foxn3 accelerates an intrinsic plasticity whose cues are not fully defined (Spijker et al., 2013).

Ultimately, a conditional, liver-limited FOXN3-deletion model will be needed to identify the mechanisms through which liver Foxn3 modulates glucagon action in fasting and to examine the effects of dietary challenges on FOXN3 function. Revealing these mechanisms may spur development of new therapeutics for treating DM2. Similarly, identifying the mechanism(s) through which glucagon normally suppresses FOXN3 expression and how the rs8004664 risk allele drives sustained FOXN3 expression could shed light on the molecular genetic cues of fasting glucose metabolism.

EXPERIMENTAL PROCEDURES

Human Subjects and Oral Glucose Tolerance Testing—Human studies were approved by the Institutional Review Board of the Mayo Clinic College of Medicine. Subjects were recruited from the Mayo Clinic Biobank and provided informed written consent. We genotyped subjects at the rs8004664 using a TaqMan SNP Genotyping Assay (Applied Biosystems assay ID C_29386020_10) and performed oral glucose tolerance testing after obtaining informed written consent (Cobelli et al., 2014; Dalla Man et al., 2005). A cohort of 402 individuals (males = 165) was recruited for oral glucose tolerance testing. Results are presented in aggregate by rs8004665 genotype.

Mouse Studies—Mouse studies were approved by the Institutional Animal Care and Use Committees (IACUC) of the University of Utah School of Medicine.

Mouse Glucagon Challenge—Seventeen-week-old C57Bl6/J male mice were purchased from Jackson Laboratory. After a 6-hr fast, animals were injected with glucagon (1 mg/kg) or normal saline. Blood was collected from the tail vein and measured with a Bayer Contour glucometer 10 minutes after glucagon injection. Twenty minutes after glucagon injection, animals were euthanized and livers were harvested.

Mouse Primary Hepatocyte Culture—Primary hepatocytes were isolated exactly as described previously (Severgnini et al., 2012; Simcox et al., 2017). Cells were treated with vehicle or 28 μM glucagon for 45 min. Proteins were extracted and subjected to immunoblot analysis.

Zebrafish Genome Editing—Zebrafish studies were approved by the IACUC of the University of Utah School of Medicine. Animals were maintained on a 14 hr light:10 hr darkness cycle. Adult female and male zebrafish were studied. All results are presented separately for each sex. Transgenic lines were used heterozygously. The CRISPR/Cas9 system was used to generate the *foxn3*^{Z111} allele on the WIK background. CRISPR guide

RNAs were designed using publicly available online programs, CRISPR design (http://crispr.mit.edu), and The Genetic Perturbation Platform Web Portal (https://portals.broadinstitute.org/gpp/public/analysis-tools/sgrna-design). The CRISPR RNA (crRNA) sequence having best "on target activity score" and least likelihood of "off target binding" was selected, synthesized, used as annealed two-part synthetic crRNA and trans-activating crRNA (tracrRNA) molecules, and delivered to zebrafish embryos as ribonucleoprotein complexes with Alt-R *Streptococcus pyogenes* Cas9 Nuclease 3NLS at the single-cell stage, following the manufacturer's instructions (Integrated DNA Technologies, Coralville, IA). Germline transmission of the mutation was confirmed with Sanger sequencing of progeny, and subsequent genotyping was done with high-resolution melt analysis (Hoshijima et al., 2016).

Zebrafish Glucagon Challenge and Fasting Blood Glucose Measurements— Human glucagon (or glycine vehicle) was injected intraperitoneally into 12 months post-fertilization (mpf) WT WIK strain animals fasted for 6 hr at a dose of 2 μg/g. Two hours later, animals were subjected to phlebotomy, glucose measurement, necroscopy, and liver RNA extraction exactly as we described (Karanth et al., 2016). For fasting measurements (and harvesting of livers for analyses), background-matched, 3 mpf WT siblings were used in studies with *foxn3*$^{z111/+}$ or *Tg*(*fabp10a:foxn3,EGFP*)^{z106} animals.

Imaging and Quantification—Background-matched WT siblings carrying *Tg*(*gcga:GFP*)^{ia1} heterozygously were used in studies with *foxn3*$^{z111/+}$ or *Tg*(*fabp10a:FOXN3,EGFP*)^{z107} animals. Embryos were fixed and permeabilized at the 7-day post-fertilization stage (when yolk is completely consumed in our facility in Salt Lake City, UT; altitude 4,500 m) in 4% paraformaldehyde, PBST (PBS+0.4% Triton X-100), and blocked in PBST + 5% Goat Serum (Sigma; G9023). Anti-GFP antibody (Torrey Pines Biolabs; TP401) was diluted 1:100; anti-phospho-S10-Histone H3 antibody (Abcam; 14955) was diluted 1:500 and incubated in PBST + 1% goat serum. Alexa 488 donkey anti-rabbit secondary (Thermo Fisher Scientific; A21206) or Alexa 488 goat anti-mouse immunoglobulin G1 (lgG1) secondary (Thermo Fisher Scientific; A21125) were diluted 1:500 and incubated in PBST + 1% goat serum. After washes in PBST, embryos were cleared in 80% glycerol for imaging with a Zeiss LSM 880 with Airyscan microscope. Images were acquired with Zen 2.3 software. Cells were counted with Imaris Image Analysis Software 9.1; maximum intensity projections were made using Fiji.

Zebrafish Plasma Glucagon Assay—Plasma glucagon was measured using a dot blot method (Matsuda et al., 2017). Plasma was collected by phlebotomy from 12 mpf animals in pools from 3 animals at a time, spotted on nitrocellulose membranes, and detected with anti-human glucagon antibodies. Because the abundance of circulating zebrafish glucagon a and glucagon b peptides are not known, results are presented as relative concentrations.

qPCR—RNA was extracted with Trizol reagent and converted into cDNA exactly as we described. Primers for qPC Rare listed inTable S2. PCR reactions were formulated following the manufacturer's instructions (PowerUp SYBR Green Master Mix; Thermo Fisher Scientific; A25742). For thermal cycling and fluorescence detection, an Agilent

Technologies Stratagene MX 3000P machine was used (Genomics Core Facility, University of Utah). The threshold (Ct) values of fluorescence for each readout was normalized to corresponding Ct values from *ef1a* (zebrafish liver) or *E2f5* (mouse liver), and fold change was calculated using the ΔΔCt method (Pfaffl, 2001).

Statistical Analysis—Data are presented as individual animal measurements (unless stated otherwise) mean ± SD for mouse and zebrafish experiments. For human experiments, mean ± SEM is shown. Statistical analyses were performed using R Studio and SigmaPlot 14.p values comparing mutant and littermate groups were calculated using one-tailed or two-tailed Student's t tests or ANOVA as indicated in the figure legends. p values of less than 0.05 were considered significant.

Supplementary Material

Refer to Web version on PubMed Central for supplementary material.

ACKNOWLEDGMENTS

This study was supported by NIH grants R01DK096710 and R56DK111494 (to A.S.), R01DK078646 and R01DK116231 (to A.V.), UM1HL098160 (to H.J.Y.), R01DK112826 (to W.L.H.), R01DK106045 (to L.O.), R01DK103930 (to C.J.V.), T32DK091317 (to J.S.), and T32DK007352 (to J.D.A.); JDRF award SRA-2016-149-Q-R (to W.L.H.); the Driving Out Diabetes – A Larry H. Miller Family Wellness Initiative postdoctoral fellowship (to S.K.); and funds from the University of Utah Molecular Medicine Program (to A.S.) and the Utah Diabetes and Metabolism Research Center (to A.S). Human studies were performed in the Mayo Clinic General Clinical Research Center (supported by UL1TR000135 from NIH; PI, Sundeep Khosla). We thank Wenbiao Chen for sharing animals and Scott Summers and Bhagirath Chaurasia for their comments and advice.

REFERENCES

Bonnefond A , and Froguel P (2015). Rare and common genetic events in type 2 diabetes: what should biologists know? Cell Metab 21, 357–368.25640731

Bozadjieva N , Blandino-Rosano M , Chase J , Dai X-Q , Cummings K , Gi-meno J , Dean D , Powers AC , Gittes GK , Riiegg MA , et al. (2017). Loss of mTORC1 signaling alters pancreatic α cell mass and impairs glucagon secretion. J. Clin. Invest 127, 4379–4393.29106387

Campbell JE , and Drucker DJ (2015). Islet α cells and glucagon-critical regulators of energy homeostasis. Nat. Rev. Endocrinol 11, 329–338.25850661

Cinti F , Bouchi R , Kim-Muller JY , Ohmura Y , Sandoval PR , Masini M , Marselli L , Suleiman M , Ratner LE , Marchetti P , and Accili D (2016). Evidence of β-cell dedifferentiation in human type 2 diabetes. J. Clin. Endocrinol. Metab 707, 1044–1054.

Cobelli C , Dalla Man C , Toffolo G , Basu R , Vella A , and Rizza R (2014). The oral minimal model method. Diabetes 63, 1203–1213.24651807

Conarello SL , Jiang G , Mu J , Li Z ,Woods J , Zycband E , Ronan J , Liu F , Roy RS , Zhu L , et al. (2007). Glucagon receptor knockout mice are resistant to diet-induced obesity and streptozotocin-mediated beta cell loss and hyperglycaemia. Diabetologia 50, 142–150.17131145

Dalla Man C , Campioni M , Polonsky KS , Basu R , Rizza RA , Toffolo G , and Cobelli C (2005).Two-hourseven-sample oral glucose tolerancetest and meal protocol: minimal model assessment of β-cell responsivity and insulin sensitivity in nondiabetic individuals. Diabetes 54, 3265–3273.16249454

Danaei G , Finucane MM , Lu Y , Singh GM , Cowan MJ , Paciorek CJ , Lin JK , Farzadfar F , Khang YH , Stevens GA , et al.; Global Burden of Metabolic Risk Factors of Chronic Diseases Collaborating Group (Blood Glucose) (2011). National, regional, and global trends in fasting plasma glucose and diabetes prevalence since 1980: systematic analysis of health examination

surveys and epidemiological studies with 370 country-years and 2–7 million participants. Lancet 378, 31–40.21705069

Dean ED , Li M , Prasad N , Wisniewski SN , Von Deylen A , Spaeth J , Maddison L , Botros A , Sedgeman LR , Bozadjieva N , et al. (2017). Interrupted glucagon signaling reveals hepatic α cell axis and role for L-glutamine in α cell proliferation. Cell Metab 25, 1362–1373.e5.28591638

Færch K , Vistisen D , Pacini G , Torekov SS , Johansen NB , Witte DR , Jonsson A , Pedersen O , Hansen T , Lauritzen T , et al. (2016). Insulin resistance is accompanied by increased fasting glucagon and delayed glucagon suppression in individuals with normal and impaired glucose regulation. Diabetes 65, 3473–3481.27504013

Fuchsberger C , Flannick J , Teslovich TM , Mahajan A , Agarwala V , Gaulton KJ , Ma C , Fontanillas P , Moutsianas L , McCarthy DJ , et al. (2016). The genetic architecture of type 2 diabetes. Nature 536, 41–47.27398621

Galsgaard KD , Winther-Sorensen M , 0rskov C , Kissow H , Poulsen SS , Vilstrup H , Prehn C , Adamski J , Jepsen SL , Hartmann B , et al. (2018). Disruption ofglucagon receptor signaling causes hyperaminoacidemia exposing a possible liver-alpha-cell axis. Am. J. Physiol. Endocrinol. Metab 314, E93–E103.28978545

Gelling RW , Du XQ , Dichmann DS , Rømer J , Huang H , Cui L , Obici S , Tang B , Holst JJ , Fledelius C , et al. (2003). Lower blood glucose, hyper-glucagonemia, and pancreatic α cell hyperplasia in glucagon receptor knockout mice. Proc. Natl. Acad. Sci. USA 100, 1438–1443.12552113

Gromada J , Franklin I , and Wollheim CB (2007). α-cells of the endocrine pancreas: 35 years of research but the enigma remains. Endocr. Rev 28,84–116.17261637

Gut P , Baeza-Raja B , Andersson O , Hasenkamp L , Hsiao J , Hesselson D , Akassoglou K , Verdin E , Hirschey MD , and Stainier DYR (2013). Whole-organism screening forgluconeogenesis identifies activators offasting metabolism. Nat. Chem. Biol 9, 97–104.23201900

Holst JJ , Wewer Albrechtsen NJ , Pedersen J , and Knop FK (2017). Glucagon and amino acids are linked in a mutual feedback cycle: the liver-α-cell axis. Diabetes 66, 235–240.28108603

Hoshijima K , Jurynec MJ , and Grunwald DJ (2016). Precise editing ofthe zebrafish genome made simple and efficient. Dev. Cell 36, 654–667.27003937

Karanth S , Zinkhan EK , Hill JT ,Yost HJ , and Schlegel A (2016). FOXN3 regulates hepatic glucose utilization. Cell Rep 15, 2745–2755.27292639

Kim J , Okamoto H , Huang Z , Anguiano G , Chen S , Liu Q , Cavino K , Xin Y , Na E , Hamid R , et al. (2017). Aminoacid transporter Slc38a5 controls glucagon receptor inhibition-induced pancreatic α cell hyperplasia in mice. Cell Metab 25, 1348–1361.e8.28591637

Larger E , Wewer Albrechtsen NJ , Hansen LH , Gelling RW , Capeau J , Deacon CF , Madsen OD , Yakushiji F , De Meyts P , Holst JJ , et al. (2016). Pancreatic α-cell hyperplasia and hyperglucagonemia due to aglucagon receptor splice mutation. Endocrinol. Diabetes Metab. Case Rep 2016,16–0081.

Li M , Dean ED , Zhao L , Nicholson WE , Powers AC , and Chen W (2015). Glucagon receptor inactivation leadsto α-cell hyperplasia in zebrafish. J. Endocrinol 227, 93–103.26446275

Longuet C , Robledo AM , Dean ED , Dai C , Ali S , McGuinness I , de Chavez V , Vuguin PM , Charron MJ , Powers AC , and Drucker DJ (2013). Liver-specific disruption ofthe murine glucagon receptor produces α-cell hyperplasia: evidence for a circulating α-cell growth factor. Diabetes 62, 1196–1205.23160527

Lotta LA , Gulati P , Day FR , Payne F , Ongen H , van de Bunt M , Gaul-ton KJ , Eicher JD , Sharp SJ , Luan J , et al.; EPIC-InterAct Consortium; Cambridge FPLD1 Consortium (2017). Integrative genomic analysis implicates limited peripheral adipose storage capacity in the pathogenesis of human insulin resistance. Nat. Genet 49, 17–26.27841877

Manning AK , Hivert MF , Scott RA , Grimsby JL , Bouatia-Naji N , Chen H , Rybin D , Liu CT , Bielak LF , Prokopenko I , et al.; DIAbetes Genetics Replication And Meta-analysis (DIAGRAM) Consortium; Multiple Tissue Human Expression Resource (MUTHER) Consortium (2012). A genome-wide approach accounting for body mass index identifies genetic variants influencing fasting glycemic traits and insulin resistance. Nat. Genet 44, 659–669.22581228

Matsuda H , Mullapudi ST , Zhang Y , Hesselson D , and Stainier DYR (2017). Thyroid hormone coordinates pancreatic islet maturation during the zebrafish larval-to-juvenile transition to maintain glucose homeostasis. Diabetes 66, 2623–2635.28698262

Parker JC , Andrews KM , Allen MR , Stock JL , and McNeish JD (2002). Glycemic control in mice with targeted disruption of the glucagon receptor gene. Biochem. Biophys. Res. Commun 290, 839–843.11785978

Pfaffl MW (2001). A new mathematical model for relative quantification in real-time RT-PCR. Nucleic Acids Res 29, e45.11328886

Safavi-Hemami H , Gajewiak J , Karanth S , Robinson SD , Ueberheide B , Douglass AD , Schlegel A , Imperial JS , Watkins M , Bandyopadhyay PK , et al. (2015). Specialized insulin is used forchemical warfare by fish-hunting cone snails. Proc. Natl. Acad. Sci. USA 112, 1743–1748.25605914

Samaan G , Yugo D , Rajagopalan S , Wall J , Donnell R , Goldowitz D , Go-palakrishnan R , and Venkatachalam S (2010). Foxn3 is essential forcraniofa-cial development in mice and a putative candidate involved in human congenital craniofacial defects. Biochem. Biophys. Res. Commun 400, 60–65.20691664

Sanghera DK , and Blackett PR (2012). Type 2 diabetes genetics: beyond GWAS. J. Diabetes Metab 3, 6948.23243555

Schuff M , Rössner A , Wacker SA , Donow C , Gessert S , and Knöchel W (2007). FoxN3 is required forcraniofacial and eye development of Xenopus laevis. Dev. Dyn 236, 226–239.17089409

Severgnini M , Sherman J , Sehgal A , Jayaprakash NK , Aubin J , Wang G , Zhang L , Peng CG , Yucius K , Butler J , and Fitzgerald K (2012). A rapid two-step method for isolation of functional primary mouse hepatocytes: cell characterization and asialoglycoprotein receptor based assay development. Cytotechnology 64, 187–195.22105762

Simcox J , Geoghegan G , Maschek JA , Bensard CL , Pasquali M , Miao R , Lee S , Jiang L , Huck I , Kershaw EE , et al. (2017). Global analysis of plasma lipids identifies liver-derived acylcarnitines as a fuel source for brown fat thermogenesis. Cell Metab 26, 509–522.e6.28877455

Solloway MJ , Madjidi A , Gu C , Eastham-Anderson J , Clarke HJ , Klja-vin N , Zavala-Solorio J , Kates L , Friedman B , Brauer M , et al. (2015). Glucagon couples hepatic amino acid catabolism to mTOR-dependent regulation of α-cell mass. Cell Rep 12, 495–510.26166562

Sørensen H , Winzell MS , Brand CL , Fosgerau K , Gelling RW , Nishimura D , and Ahren B (2006). Glucagon receptor knockout mice display increased insulin sensitivity and impaired β-cell function. Diabetes 55, 3463–3469.17130493

Spijker HS , Ravelli RBG , Mommaas-Kienhuis AM , van Apeldoorn AA , Engelse MA , Zaldumbide A , Bonner-Weir S , Rabelink TJ , Hoeben RC , Clevers H , et al. (2013). Conversion of mature human β-cells into glucagon-producing α-cells. Diabetes 62, 2471–2480.23569174

Talchai C , Xuan S , Lin HV , Sussel L , and Accili D (2012). Pancreatic β cell dedifferentiation as a mechanism ofdiabetic β cell failure. Cell 150,1223–1234.22980982

Ye L , Robertson MA , Hesselson D , Stainier DYR , and Anderson RM (2015). Glucagon is essential for alpha cell transdifferentiation and beta cell neogenesis. Development 142, 1407–1417.25852199

Zecchin E , Filippi A , Biemar F , Tiso N , Pauls S , Ellertsdottir E , Gnügge L , Bortolussi M , Driever W , and Argenton F (2007). Distinct delta and jagged genes control sequential segregation of pancreatic cell types from precursor pools in zebrafish. Dev. Biol 301, 192–204.17059815

Highlights

- Glucagon lowers FOXN3 expression in liver
- Deletion of FOXN3 lowers fasting blood glucose in zebrafish
- Deletion of FOXN3 decreases the number of α cells in the endocrine pancreas
- The FOXN3 hyperglycemia risk allele blunts glucagon suppression during glucose challenge

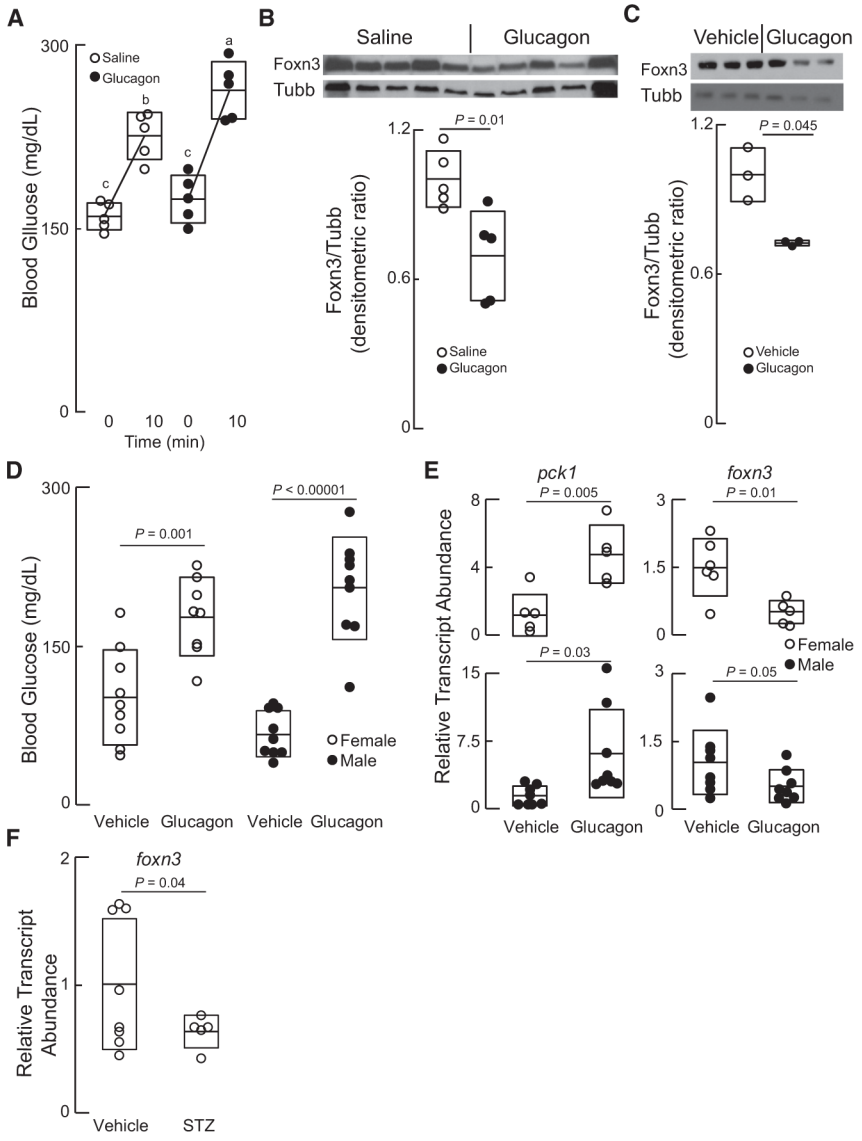

Figure 1. Glucagon Regulates Liver Foxn3 Expression in Mice and Zebrafish

(A) A glucagon challenge test was performed in mice; blood glucose was measured at baseline and 10 min after injection of glucagon or vehicle (PBS). Mean, SD, n, and significance groups ($p < 0.01$ in one-sided ANOVA) are shown.

(B) Foxn3 protein abundance was quantified with immunoblot analysis of liver homogenates from fed and fasted mouse livers. Mean, SD, n, and p values for a 2-sided Student's t test are shown.

(C) Foxn3 protein abundance was quantified with immunoblot analysis of mouse primary hepatocytes treated with vehicle or glucagon. Mean, SD, n, and p values for a 2-sided Student's t test are shown.

(D) Blood glucose in adult zebrafish 2 hr after injection with vehicle or human glucagon. Mean, SD, n, and p values for a 2-sided Student's t test are shown.

(E) Liver *pck1* and *foxn3* transcript abundance two hours after injection of human glucagon. Mean, SD, n, and p values for a 2-sided Student's t test are shown. See also Table S1.

(F) Liver *foxn3* transcript in zebrafish rendered hyperglycemic with STZ; 1-sided Student's t test.

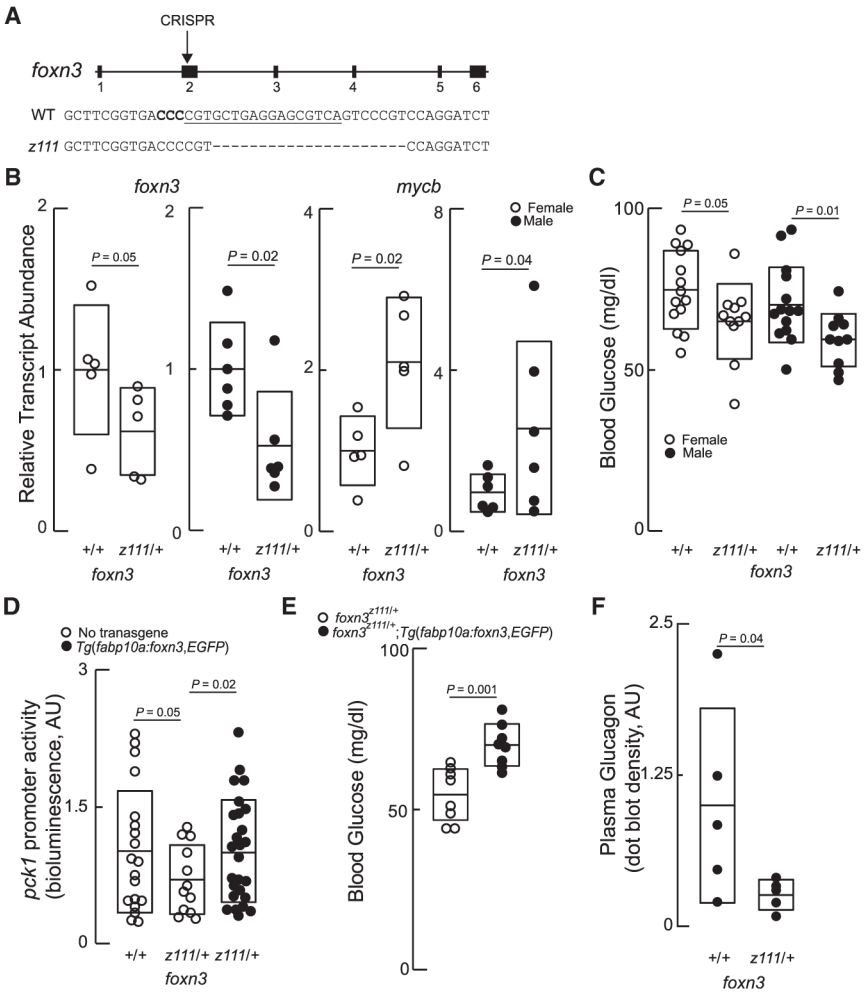

Figure 2. Mutation of Zebrafish *foxn3* Decreases Fasting Blood Glucose and Glucagon and Liver Gluconeogenic Gene Expression

(A) CRISPR/Cas9-generated *foxn3* mutant with an in-frame 7-codon deletion, removing residues 81–87 from the Forkhead Box (strain *z111*). The CRISPR guide RNA sequence is underlined; the protospacer adjacent motif is in bold font.

(B) Decreased *foxn3* transcript and increased *mycb* transcript abundance in $fon3^{Z111/+}$ livers.

(C) Decreased fasting blood glucose in both female and male 3 months post-fertilization adult *foxn3* mutants maintained on regular diets. Two-tailed t test is shown.

(D) Decreased *pck1* luciferase gene reporter activity in *foxn3* mutants, which is rescued by the liver-specific overexpression of *foxn3*. Mean, SD, n, and p values for a 1-sided Student's t test are shown.

(E) Liver-specific overexpression of *foxn3* increases blood glucose in male $foxn3^{z111/+}$ mutants; 2-sided Student's t test.

(F) Decreased plasma glucagon in *foxn3* mutants; 1-sided Student's t test.

Mean, SD, n, and p values are shown in (B)–(E). For (F), each dot reflects plasma pooled from 3 animals per dot blot sample (i.e., n = 15 for each group); mean, SD, and p are shown. See also Table S1 and Figure S1.

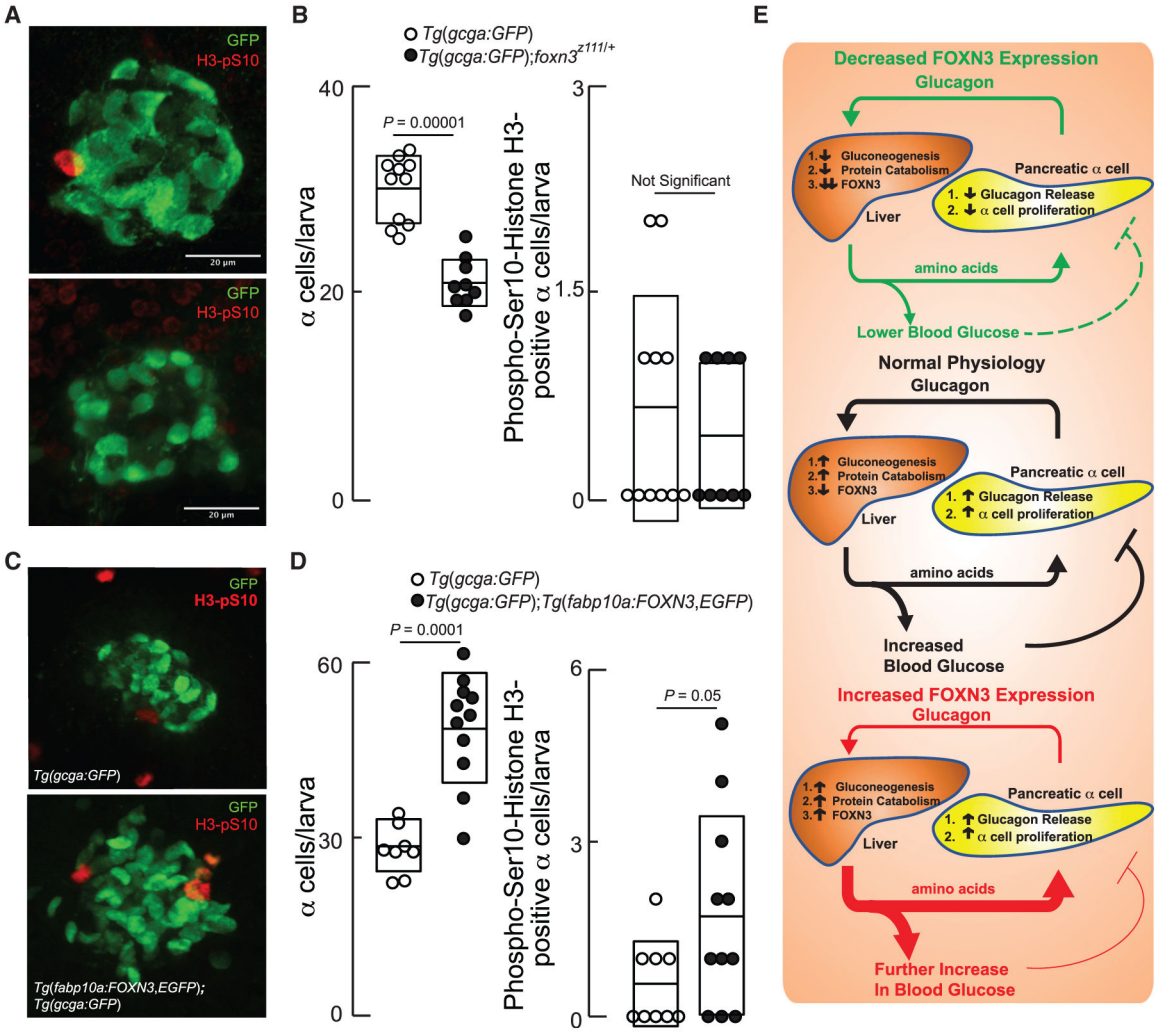

Figure 3. Liver Foxn3 Regulates α Cell Mass

(A) Representative whole-mount images and quantification of α cells (GFP) and proliferating α cells (stained with anti-phospho-Ser10-histone H3 antibody [H3-pS10]) in WT (*Tg*(*gcga:GFP*)) and *foxn3* mutant (*foxn3*$^{z111/+}$; *Tg*(*gcga:GFP*)) larvae. (B) Quantification of (A). Mean, SD, n, and p values in a 2-sided Student's t test are shown. The scale bars represent 20 μm. (C) Representative whole-mount images and quantification of a cells (GFP) and proliferating a cells (stained with pS10-H3 antibody) in WT (*Tg*(*gcga:GFP*)) and *Tg* (*fabp10a:FOXN3,EGFP*);(*Tg*(*gcga:GFP*)) transgenic larvae. (D) Quantification of (C). Mean, SD, n, and p values in a 2-sided Student's t test are shown. The scale bars represent 25 μm. See also Figure S1. (E) Model of how FOXN3 is regulated by and regulates glucagon. Hypoglycemia triggers physiological release of glucagon from pancreatic α cells (middle panel). Glucagon acts on liver to promote gluconeogenesis and protein catabolism (liberating gluconeogenic amino acids). Glycogen synthesis is suppressed by glucagon as well (not shown). Finally, glucagon signaling normally suppresses expression of the transcriptional regulator FOXN3. Glucagon-directed glucose production in liver leads to export of glucose into the circulation; the increased blood glucose suppresses

further glucagon release from pancreatic α cells, closing the feedback loop. In human carriers of the hyperglycemia risk allele of the rs8004664 variation (and transgenic zebrafish overexpressing Foxn3 in the liver), FOXN3 expression is increased (lower panel) and suppression of further glucagon secretion is blunted (thin red line). This causes blood glucose to increase in fasting because gluconeogenesis is increased (Karanthet al., 2016). Conversely, deletion of Foxn3 decreased blood glucose (upper panel), and less feedback to α cells is needed to suppress glucagon secretion (dashed green line). Whether Foxn3 regulates amino acid catabolism is not known. Similarly, the role of liver Foxn3 in regulating pancreatic α cell specification, differentiation, proliferation, and survival needs to be elucidated. This model is inspired by the model of Holst et al. (2017).

Table 1.

Anthropometric Data of Human Subjects Studied

	Mean ± SEM	Range (Min–Max)
Age (years)	51 ± 1	12–84
Height(centimeters)	168.4 ± 0.5	77.5–192.4
Mass (kg)	80.3 ± 0.9	48.4–177.8
BMI (kg/m^2)	27.9 ± 0.2	19.0–44.9
Lean mass (kg)	45.3 ± 0.6	28.5–77.2
% body fat	40.9 ± 0.7	15.6–62.0

Table 2.

Oral Glucose Tolerance Test Parameters

rs8004664 Genotype	G|G (n = 76)	G|A (n = 195)	A|A (n = 131)	p Value (Univariate, Multivariate)	
Fasting glucose (mg/dL)	97 ± 1	99 ± 1	101 ± 1	0.05	0.10
Peak glucose	187 ± 4	188 ± 2	190 ± 3	0.46	0.61
Glucose 120 min	145 ± 4	145 ± 3	148 ± 3	0.70	0.51
AUC glucose	19,500 ± 800	19,200 ± 300	19,200 ± 300	0.89	0.89
AAB glucose	7,800 ± 800	7,300 ± 300	7,000 ± 200	0.57	0.65
Fasting insulin (μIU/mL)	6.5 ± 0.6	7.7 ± 0.6	7.0 ± 0.5	0.40	0.32
Peak insulin	76.9 ± 5.4	86.1 ± 5.2	81.5 ± 5.1	0.54	0.55
AUC insulin	6,000 ± 400	6,300 ± 300	6,200 ± 400	0.80	0.84
AAB insulin	5,200 ± 400	5,400 ± 300	5,300 ± 300	0.88	0.91
Fasting C-peptide (ng/mL)	0.7 ± 0.1	0.8 ± 0.1	0.8 ± 0.1	0.42	0.46
Peak C-peptide	3.7 ± 0.1	3.8 ± 0.1	3.8 ± 0.1	0.76	0.82
AUC C-peptide	320 ± 10	338 ± 9	328 ± 9	0.55	0.58
AAB C-peptide	234 ± 10	241 ± 6	235 ± 7	0.73	0.74
Insulin sensitivity	15 ± 1	14 ± 1	14 ± 1	0.85	0.94
Basal ϕ^a	7.8 ± 0.4	8.5 ± 0.3	8.1 ± 0.3	0.46	0.41
First phase ϕ	640 ± 50	690 ± 30	730 ± 40	0.35	0.44
Second phase ϕ	48 ± 3	49 ± 2	51 ± 2	0.59	0.68
Total ϕ	55 ± 3	54 ± 3	58 ± 3	0.88	0.63
Disposition index	1,240 ± 150	1,150 ± 70	1,230 ± 120	0.75	0.63
Fasting glucagon (pg/mL)	78 ± 2	77 ± 2	78 ± 2	0.86	0.66
Nadir glucagon	56 ± 2	53 ± 1	57 ± 2	0.09	0.09
AUC glucagon	7,900 ± 300	7,600 ± 200	8,200 ± 300	0.17	0.18
ABB glucagon	−1,570 ± 170	−1,590 ± 120	−1,170 ± 190	0.11	0.04
Creatinine (mg/dL)	0.90 ± 0.03	0.86 ± 0.02	0.92 ± 0.02	0.11	0.23

Univariateand multivariate (adjusting for age, weight, and sex) results are present. Data are presented as mean ± SEM; n and p values are shown. AAB, area above baseline; ABB, area below baseline; AUC, area under the curve.

[a] β cell responsivity to glucose (Phi).